

Sparsely Aggregated Convolutional Networks

Ligeng Zhu¹ Ruizhi Deng¹ Michael Maire² Zhiwei Deng¹ Greg Mori¹ Ping Tan¹

¹Simon Fraser University ²Toyota Technological Institute at Chicago
{lykenz,ruizhid,zhiweid,mori,pingtan}@sfu.edu, mmair@ttic.edu

Abstract. We explore a key architectural aspect of deep convolutional neural networks: the pattern of internal skip connections used to aggregate outputs of earlier layers for consumption by deeper layers. Such aggregation is critical to facilitate training of very deep networks in an end-to-end manner. This is a primary reason for the widespread adoption of residual networks, which aggregate outputs via cumulative summation. While subsequent works investigate alternative aggregation operations (*e.g.* concatenation), we focus on an orthogonal question: which outputs to aggregate at a particular point in the network. We propose a new internal connection structure which aggregates only a sparse set of previous outputs at any given depth. Our experiments demonstrate this simple design change offers superior performance with fewer parameters and lower computational requirements. Moreover, we show that sparse aggregation allows networks to scale more robustly to 1000+ layers, thereby opening future avenues for training long-running visual processes.

1 Introduction

As convolutional neural networks have become a central component of many vision systems, successive improvements in their basic design have quickly permeated the field. This is exemplified by a series of popular CNN architectures, most notably: AlexNet [1], VGG [2], Inception [3,4], ResNet [5,6], and DenseNet [7]. Though initially targeted to image classification, each of these designs has quickly slotting into serving the role of a backbone across a broader range of vision tasks, including object detection [8,9] and semantic segmentation [10,11,12]. Advances in the backbone architecture consistently translate into corresponding performance boosts to these downstream tasks.

We examine a core design element, internal aggregation links, of the recent residual (ResNet [5]) and dense (DenseNet [7]) network architectures. Though vital to the success of these architectures, we demonstrate that the specific structure of aggregation in current networks is at a suboptimal design point. DenseNet, considered state-of-the-art, actually wastes capacity by allocating too many parameters and too much computation along internal aggregation links.

We suggest a principled alternative design for internal aggregation structure, applicable to both ResNets and DenseNets. Our design is a sparsification of the default aggregation structure. In both ResNet and DenseNet, the input to a particular layer is formed by aggregating the output of all previous layers. We switch

from this full aggregation topology to one in which only a subset of previous outputs are linked into a subsequent layer. By changing the number of incoming links to be logarithmic, rather than linear, in the overall depth of the network, we fundamentally reduce the growth of parameters in our resulting analogue of DenseNet. Experiments reveal our design to be uniformly advantageous:

- On standard tasks, such as image classification, SparseNet, our sparsified DenseNet variant, is more efficient than both ResNet and DenseNet. This holds for measuring efficiency in terms of both parameters and operations (FLOPs) required for a given level of accuracy. A much smaller SparseNet model matches the performance of the highest accuracy DenseNet.
- In comparison to DenseNet, the SparseNet design scales in a robust manner to instantiation of extremely deep networks of 1000 layers and beyond. Such configurations magnify the efficiency gap between DenseNet and SparseNet.
- Our aggregation pattern is equally applicable to ResNet. Switching ResNet to our design preserves or improves ResNet’s performance properties. This suggests that aggregation topology is a fundamental consideration of its own, decoupled from other design differences between ResNet and DenseNet.

Section 4 provides full details on these experimental results. Prior to that, Section 2 relates background on the history and role of skip or aggregation links in convolutional neural networks. It places our contribution in the context of much of the recent research focus on CNN architecture.

Section 3 presents the details of our sparse aggregation strategy. Our approach occupies a previously unexplored position in aggregation complexity between that of standard CNNs and FractalNet [13] on one side, and ResNet and DenseNet on the other. Taken together with our experimental results, sparse aggregation appears to be a simple, general improvement that is likely to filter into the standard CNN backbone design. Section 5 concludes with a synthesis of these observations, and discussion of potential future research paths.

2 Related Work

Modern CNN architectures usually consist of a series of convolutional, ReLU, and batch normalization [14] layers, interspersed with occasional max-pooling and subsampling operations. Much prior research focuses on optimizing for parameter efficiency within convolution layers, for example, via dimensionality reduction bottlenecks [15,5,6], grouped convolution [16,17], or weight compression [18]. These efforts all concern design at a micro-architectural level, optimizing structure that fits inside a repeating building block containing at most a few layers.

At a macro-architectural level, skip connections have emerged as a common and useful design motif. Such connections route outputs of earlier CNN layers directly to the input of far deeper layers, skipping over the sequence of intermediate layers. Some deeper layers thus take input from multiple paths: the

usual sequential path as well as these shortcut connections. Multiple intuitions motivate inclusion of skip connections, and may share a role in explaining their effectiveness.

2.1 Skip Connections for Features

Predicting a detailed labeling of a complicated visual scene may require understanding it at multiple levels of abstraction, from edges and textures to object categories. Taking the (plausible) view that a CNN learns to compute increasingly abstract visual representations when going from shallower to deeper layers, then skip connections can provide a pathway for assembling features that combine many levels of abstraction. Building in such connections alleviates the burden of having to learn to store and maintain a feature computed early that the network needs again later.

This intuition motivates the skip-connection structures found in many semantic segmentation CNNs. Fully convolutional networks [19] upsample and combine several layers of a standard CNN, to act as input to a final prediction layer. Hypercolumn networks [20] similarly wire intermediate representations into a concatenated penultimate feature descriptor. Rather than use the end of the network as the sole destination for skip links, encoder-decoder style architectures such as SegNet [21] and U-Net [22] introduce internal skip links between encoder and decoder layers of corresponding spatial resolutions. Such internal feature aggregation, though with different connectivity, is also exploited for the purpose of making very deep networks trainable.

2.2 Training Very Deep Networks

Training deep networks end-to-end via stochastic gradient descent requires back-propagating a signal through all layers of the network. Beginning with random parameter initialization, the gradient received by earlier layers from a loss at the end of the network will be noisier than that received by deeper layers. This issue worsens with deeper networks, making them more challenging to train. Attaching additional loss signals directly to intermediate layers [23,3] is one strategy for ameliorating this problem.

Highway networks [24] and residual networks [5] (ResNets) offer a more elegant solution, preserving the ability to train from a single loss by adding skip connections to the network architecture. The addition of skip connections shortens the effective path length between early network layers and an informative loss. Highway networks add a gating mechanism, while residual networks implement skip connections by summing outputs of all previous layers. The effectiveness of the later strategy is cause for its current widespread adoption.

Fractal networks [13] demonstrate an alternative skip connection structure for training very deep networks. The accompanying analysis reveals skip connections function as a kind of scaffold that supports the training processes. Under special conditions, the FractalNet skip connections can be discarded after training.

DenseNet [7] builds most directly on ResNet, by simply switching the operational form of skip connections from summation to concatenation. DenseNets maintain the same aggregation topology as ResNets, in that the outputs of all previous layers are concatenated.

2.3 Architecture Search

The dual motivations of building robust representations and enabling end-to-end training drive inclusion of internal aggregation links, but do not dictate an optimal procedure for doing so. Absent insight into optimal design methods, one can treat architectural details as hyperparameters over which to optimize [25]. Training of a single network can then be wrapped as a step in larger search procedure that varies network design. However, naive approaches to such search can be prohibitively expensive.

Furthermore, it is unclear whether skip link topology is an important hyperparameter over which to search. Our proposed aggregation topology is motivated by a simple construction, and as shown in Section 4 significantly outperforms prior hand-designed structures. Perhaps our topology is near optimal and will free architecture search to focus on more consequential hyperparameters.

2.4 Concurrent Work

Concurrent, yet unpublished, work in the form of an arXiv preprint [26] proposes a modification of DenseNet similar to our SparseNet design. Our work is independent of this concurrent effort. Moreover, we make distinct contributions in comparison:

- Our SparseNet image classification results are substantially better than those reported in [26] and represent an actual improvement over the DenseNet baseline. It is unclear why [26] does not demonstrate similar performance and efficiency improvements.
- We explore sparse aggregation topologies in a more general setting, showing application to both ResNet and DenseNet, whereas [26] is proposed as a specific change to DenseNet.
- We experiment with networks in extreme configurations (*e.g.* 1000 layers) in order to highlight robustness of our design principles in regimes where current baselines begin to break down.

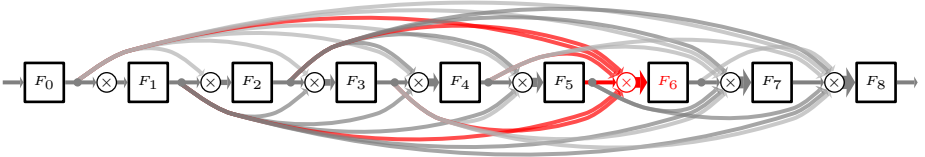
3 Aggregation Architectures

Figure 1 sketches our proposed sparse aggregation architecture alongside the dominant ResNet [7] and DenseNet [7] designs, as well as the previously proposed FractalNet [13] alternative to ResNet. This macro-architectural view abstracts away details such as the specific functional block $F(\cdot)$, parameter counts and feature dimensionality, and the aggregation operator \otimes . As our focus is on a

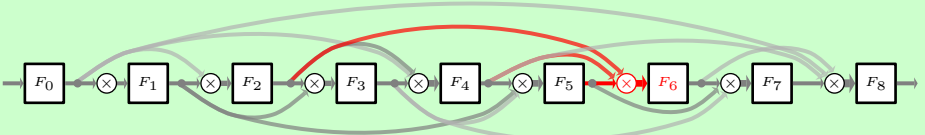
(a) Dense Aggregation (ResNet / DenseNet Topology)



(b) Dense Aggregation: Equivalent Exploded View of (a)



(c) Sparse Aggregation (Our Proposed Topology)



(d) Fractal Aggregation (FractalNet)

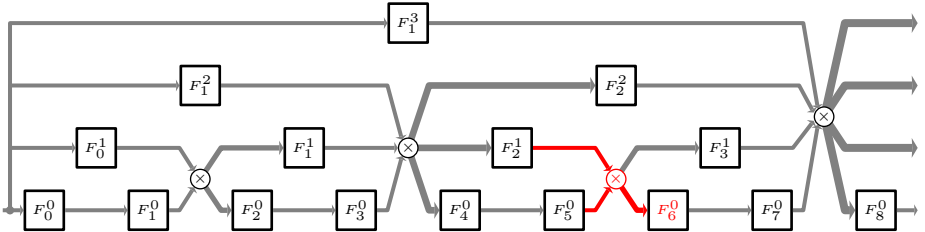


Fig. 1. Aggregation topologies. Our proposed sparse aggregation topology devotes less machinery to skip-connection than DenseNet [7], but more than FractalNet [13]. This is apparent by comparing the exploded view (b) of the ResNet [5] or DenseNet topology (a), as well as the fractal topology (d), with our proposal (c). All of these architectures are describable in terms of a basic parameterized functional block $F(\cdot)$ (e.g. convolution-ReLU-batchnorm), an aggregation operator \otimes , and a connection pattern. For ResNet, \otimes is addition $+$; for DenseNet, \otimes is concatenation \oplus ; for FractalNet \otimes is averaging $\overline{+}$. Note how the compact view (a) feeds the result of one aggregation into the next; the exploded view (b) of DenseNet is the correct visualization for comparison to (c) and (d). For a network of depth N , dense aggregation requires $O(N^2)$ connections, sparse aggregation $O(N \log(N))$, and fractal aggregation $O(2N)$. These differences are visually apparent by comparing incoming links at a common depth. For example, compare the density of the (highlighted red) links into layer $F_6(\cdot)$.

novel aggregation topology, experiments in Section 4 match these other details to those of ResNet and DenseNet baselines.

We define a network with a sparse aggregation structure to be a sequence of blocks $F_l(\cdot)$ operating on input x , with the output of layer ℓ computed as:

$$y_0 = F_0(x) \tag{1}$$

$$y_\ell = F_l(\otimes(y_{\ell-c^0}, y_{\ell-c^1}, y_{\ell-c^2}, y_{\ell-c^3}, \dots, y_{\ell-c^k})) \tag{2}$$

where c is a positive integer and k is the largest non-negative integer such that $c^k \leq \ell$. \otimes is the aggregation function. This amounts to connecting each layer to previous layers at exponentially increasing offsets. Contrast with ResNet and DenseNet, which connect each layer to all previous layers according to:

$$y_\ell = F_l(\otimes(y_{\ell-1}, y_{\ell-2}, y_{\ell-3}, y_{\ell-4}, \dots, y_0)) \tag{3}$$

For a network of total depth N , the full aggregation strategy of ResNet and DenseNet introduces N incoming links per layer, for a total of $O(N^2)$ connections. In contrast, sparse aggregation introduces no more than $\log_c(N)$ incoming links per layer, for a total of $O(N \log(N))$ connections.

Our sparse aggregation strategy also differs from FractalNet’s aggregation pattern. The FractalNet [13] design places a network of depth N in parallel with networks of depth $\frac{N}{2}, \frac{N}{4}, \dots, 1$, making the total network consist of $2N$ layers. It inserts occasional join (aggregation) operation between these parallel networks, but does so with such extreme sparsity that the total connection count is still dominated by the $O(2N)$ connections in parallel layers.

Our proposed sparse connection pattern is therefore sparser than ResNet or DenseNet, yet denser than FractalNet. It occupies a previously unexplored point that represents a fundamentally different scaling rate of skip-connection density with network depth.

3.1 Potential Drawbacks of Dense Aggregation

The ability to train networks with depth greater than 100 layers using DenseNet and ResNet architectures can be partially attributed to their feature aggregation strategies. As discussed in Section 2, skip links serve as a training scaffold, allowing each layer to be directly supervised by the final output layer, and aggregation may help transfer useful features from shallower to deeper layers.

However, dense feature aggregation comes with several potential drawbacks. These drawbacks appear in different forms in the ResNet-styled aggregation by summation and the DenseNet-styled aggregation by concatenation, but share a common theme of over-constraining or over-burdening the system.

Theoretically speaking, it is impossible to disentangle components of a set of features after taking their sum. As the depth of a residual network grows, the number of features maps aggregated grows linearly. Later features may corrupt or wash-out of the information carried by earlier feature maps. This information loss caused by summation could partially explain the saturation of ResNet performance when the depth exceeds 1000 layers [5]. This way of combining features

is also hard-coded in the design of ResNets, giving the model little flexibility to learn more expressive combination strategies. This constraint may be the reason that ResNet layers tend to learn perform incremental feature updates [27].

In contrast, the aggregation style of DenseNets combines the features through direct concatenation which preserves the original form of the previous features. Concatenation allows each subsequent layer a clean view of all previously computed features, making feature reuse trivial. This factors may contribute to the better parameter-performance efficiency of DenseNet over ResNet.

But aggregation by concatenation has its own problems as well: the number of skip connections and required parameters grows at the asymptotic rate of $O(N^2)$ where N is the network depth. This asymptotically quadratic growth means that a significant portion of the network is devoted to processing previously seen feature representations. Each layer contributes only a few new outputs to an ever-widening concatenation of stored state. Experiments show that it is hard for the model to make full use of all the parameters and dense skip connections. In the original DenseNet work [7], a large fraction of the skip connections have average absolute weights of convolution filters close to zero. This result implies that the feature maps aggregated by these skip connections are not fully exploited.

The pitfalls of dense feature aggregation in both DenseNet and ResNet are caused by the linear growth in the number of features aggregated with respect to the depth. Variants of ResNet and DenseNet, including the post-activation ResNets [6], mixed-link networks [28] and dual-path networks [29] can all be derived from the same dense aggregation, differing only by aggregation operator. They thus inherit potential limitations of the dense aggregation topology.

3.2 Properties of Sparse Aggregation

We would like to maintain the power of short gradient paths for training, while avoiding the potential drawbacks of dense feature aggregation. SparseNets do, in fact, have shorter gradient paths than architectures without aggregation.

In plain feed-forward networks, there is only one path from a layer to a previous layer with offset S and the length of the path is $O(S)$. The length of the shortest gradient path is constant in dense aggregation networks like ResNet and DenseNet. However, the cost of maintaining a gradient path with $O(1)$ length between any two layers is the linear growth of the count of aggregated features. By aggregating features only from layers with exponential offset the length of the shortest gradient path between two blocks with offset S is bounded by $O((c - 1) \log(S))$. Here, c is again the base of the exponent governing the sparse connection pattern.

It is also worth noting that the number of predecessor outputs gathered by the ℓ^{th} block is $O(\log(\ell))$, as it only reaches predecessors with exponential offsets. Therefore, the total number of skip connections is

$$\sum_{\ell=1}^N \lfloor \log_c \ell \rfloor = O(N \log N) \quad (4)$$

where N is the number of basic blocks (depth) of the network. The number of parameters are $O(N \log N)$ and $O(N)$, respectively, for aggregation by concatenation and aggregation by summation. Table 1 summarizes these properties.

4 Experiments

We demonstrate the effectiveness SparseNets as a drop-in replacement (and upgrade) for state-of-the-art networks with dense feature aggregation, namely ResNets [5,6] and DenseNets [7], through image classification tasks on the CIFAR [30] and ImageNet datasets [31]. Except for the difference between the dense and sparse aggregation topologies, we set all other SparseNet hyperparameters to be the same as the corresponding ResNet or DenseNet baseline.

For some large models, image classification accuracy appears to saturate when we continue increasing model depth or output channel number. It is likely such saturation is not due to model capacity limits, but rather both our model and baselines reach diminishing returns given the dataset size and task complexity. We are interested not only in absolute accuracy, but also parameter-accuracy and FLOP-accuracy efficiency.

We implement our models in PyTorch framework [32]. For optimization, we use SGD with Nesterov momentum 0.9 and weight decay 0.0001. We train all models from scratch using He *et al.*'s initialization scheme [33]. All networks were trained using NVIDIA GTX 1080 Ti GPUs.

4.1 Datasets

CIFAR Both the CIFAR-10 and CIFAR-100 datasets [30] have 50,000 training images and 10,000 testing images with size of 32×32 pixels. CIFAR-10 (C10) and CIFAR-100 (C100) have 10 and 100 classes respectively. Our experiments use standard data augmentation, including mirroring and shifting, as done in [7]. The mark + beside C10 or C100 in results tables indicates this data augmentation scheme. As preprocessing, we normalize the data by the channel mean and standard deviation. Following the schedule from the Torch implementation

	Parameters	Shortest Gradient Path	Aggregated Features
Plain	$O(N)$	$O(N)$	$O(1)$
ResNets	$O(N)$	$O(1)$	$O(\ell)$
DenseNets	$O(N^2)$	$O(1)$	$O(\ell)$
SparseNets (sum)	$O(N)$	$O(\log(N))$	$O(\log \ell)$
SparseNets (concat)	$O(N \log N)$	$O(\log(N))$	$O(\log \ell)$

Table 1. SparseNet properties. We compare architecture-induced scaling properties for networks of depth N and for individual layers located at depth ℓ .

of ResNet [34]¹, our learning rate starts from 0.1 and is divided by 10 at epoch 150 and 225.

ImageNet The ILSVRC 2012 classification dataset [31] contains 1.2 million images for training, and 50K for validation, from 1000 classes. For a fair comparison, we adopt the standard augmentation scheme for training images as in [34,7,5]. Following [5,7], we report classification errors on the validation set with single crop of size 224×224 .

Architecture	Depth	Params	C10+	C100+
ResNet [5]	110	1.7M	6.61	-
ResNet(pre-activation)[5]	164	1.7M	5.46	24.33
ResNet(pre-activation)[5]	1001	10.2M	4.62	21.42*
Wide ResNet [35]	16	11.0M	4.81	22.07
FractalNet [36]	21	38.6M	5.52	23.30
DenseNet (k=12)[7]	40	1.1M	5.39*	24.79*
DenseNet (k=12)[7]	100	7.2M	4.28*	20.97*
DenseNet (k=24)[7]	100	28.3M	4.04*	19.61*
DenseNet (k=16, 32, 64)[7]	100	61.1M	4.31*	20.6*
DenseNet (k=32, 64, 128)[7]	100	241.6M	N/A	N/A
DenseNet-BC (k=24)[7]	250	15.3M	3.65	17.6
DenseNet-BC (k=40)[7]	190	25.6M	3.75*	17.53*
DenseNet-BC (k=16, 32, 64)[7]	100	7.9M	4.02*	19.55*
DenseNet-BC (k=32, 64,128)[7]	100	30.5M	3.92*	18.71*
SparseNet (k=12)	40	0.8M	5.13	24.65
SparseNet (k=24)	100	2.5M	4.64	22.41
SparseNet (k=36)	100	5.7M	4.34	20.50
SparseNet (k=16, 32, 64)	100	7.2M	4.11	19.49
SparseNet (k=32, 64, 128)	100	27.7M	3.88	18.80
SparseNet-BC (k=24)	100	1.5M	4.03	22.12
SparseNet-BC (k=36)	100	3.3M	3.91	20.31
SparseNet-BC (k=16, 32, 64)	100	4.4M	3.43	19.71
SparseNet-BC (k=32, 64, 128)	100	16.7M	3.22	17.71

Table 2. CIFAR classification performance. We show classification error rate for SparseNets compared to DenseNets, ResNets, and their variants. Results marked with a * are from our implementation. Datasets marked with + indicates use of standard data augmentation (translation and mirroring).

4.2 Results on CIFAR

Table 2 reports experimental results on CIFAR [30]. The best SparseNet closely matches the performance of the state-of-the DenseNet. In these experiments, we instantiate SparseNet to be exactly the same as the correspondingly named DenseNet, but with sparser aggregation structure (some connections removed). The parameter k indicates feature growth rates (how many new feature channels each layer produces), which we match to the DenseNet baseline. Model whose names end with BC use the bottleneck compression structure, as in the original DenseNet paper. As SparseNet does fewer concatenations than DenseNet, the same feature growth rate produces models with fewer overall parameters. Remarkably, for many of the corresponding 100 layer models, SparseNet performs as well or better than DenseNet, while having substantially fewer parameters.

¹ <https://github.com/facebook/fb.resnet.torch>

Model	Depth	Params	CIFAR 100+	Model	Depth	Params	CIFAR 100+
ResNet	56	0.59M	27.00	DenseNet(k=12)	40	1.10M	24.79
	110	1.15M	24.70		100	7.20M	20.97
	200	2.07M	23.10		400	117M	N/A
	1001	10.33M	21.42	DenseNet-BC(k=24)	250	25.6M	17.6
	2000	20.62M	22.76		400	216.3M	N/A
SparseNet[+]	56	0.59M	27.70	DenseNet-BC(k=4)	400	1.10M	32.94
	110	1.15M	26.10		1001	6.63M	28.50
	200	2.07M	25.77	SparseNet[⊕] -BC (k=12)	100	0.40M	27.99
	1001	10.33M	22.10		400	1.70M	24.41
	2000	20.62M	21.01		1001	4.62M	22.10

Table 3. Depth scalability on CIFAR. *Left:* ResNets and their sparsely aggregated analogue SparseNets[+]. *Right:* DenseNets and their corresponding sparse analogues SparseNets[⊕]. Observe that ResNet and all SparseNet variants of any depth exhibit robust performance. DenseNets suffer an efficiency drop when stretched too deep.

4.3 Going Deeper with Sparse Connections

Table 3 shows results of pushing architectures to extreme depth. While Table 2 explored only the SparseNet analogue of DenseNet, we now explore switching both ResNet and DenseNet to sparse aggregation structures, and denote their corresponding SparseNets by SparseNet[+] and SparseNet[⊕], respectively.

Both ResNet and SparseNet[+] demonstrate better performance on CIFAR100 their depth increases from 56 to 200. The gap between the performance of ResNet and SparseNet[+] initially enlarges the depth increases. However, it narrows as the depth reaches 1001 layers and the performance of SparseNet[+]-2000 surpasses ResNet-2000. SparseNet[+] appears better able to scale to depths over 1000 than ResNet.

Similar to ResNet and SparseNet[+], the performance of DenseNet and SparseNet[⊕] also becomes better as the depth increases as is shown. The performance of DenseNet is also affected by the growth rate. However, the parameter count of DenseNet explodes as we increase the depth to 400, even with growth rate of 12. Bottleneck compression layers have to be adopted and the number of filters in each layer has to be significantly reduced if we want to go deeper. We experimented with DenseNet with depth greater than 1000 after adopting bottleneck compression (BC) structure and using a growth rate of 4. But, the performance is far from satisfying. In contrast, building SparseNet[⊕] with more than 1000 layers is practical and memory-efficient. We can easily build SparseNet[⊕] with depth greater than 400 with BC structure and growth rate of 12. It demonstrates better performance than DenseNet-1001.

An important advantage of SparseNet[⊕] over DenseNet is that the number of previous layers aggregated can be bounded a small integer even when the depth of the network is over 1000 due to slow growing rate of the logarithm function. This feature not only permits SparseNet[⊕] to go deeper, but allow us

to explore hyperparameters of SparseNet $[\oplus]$ with more flexibility on depth and each layer’s number of filters.

We also observe that SparseNets $[\oplus]$ generally has better parameter efficiency than SparseNets $[+]$. For example, the error rate of SparseNet $[+]$ -1001 and SparseNet $[\oplus]$ -1001 are (coincidentally) both 22.10 on CIFAR 100 datasets. However SparseNet $[\oplus]$ -1001 requires less than half the number of parameters of SparseNet $[+]$ -1001. Similar trends are also seen in the comparison between SparseNet $[+]$ -400 and SparseNet $[\oplus]$ -100. The DenseNet *vs.* ResNet advantage of preserving features via concatenation (over summation) also migrates to the sparse aggregation pattern.

4.4 Efficiency of SparseNet $[\oplus]$

Thanks to its better flexibility and parameter efficiency, we conducted the following experiments on SparseNet $[\oplus]$ to further explore its parameter efficiency by varying the depth and number of filters of SparseNets $[\oplus]$. As the number of features in each layer aggregates grows slowly and is almost a constant in one stage, we also double the number of filters across stages, following the approach of ResNets. These experiment results are presented in Table 2.

There are two obvious general trends in the results. First, SparseNet $[\oplus]$ usually requires fewer parameters than DenseNet when they have close performance. Most notably, DenseNet $N = 190, k = 40$ requires 25.6 million parameters to achieve error rate 17.53% on CIFAR100+, while SparseNet $[\oplus]$ can achieve a similar error rate 17.71% under setting $N = 100, k = 32, 64, 128$ with only 16.72 million parameters. The performance of SparseNet-BC $N = 100, k = \{32, 64, 128\}$ 19.71 is close to the performance of DenseNet BC $N = 190, k = 40$ but requires 1 million fewer parameters.

Second, when both networks have less than 15 million parameters, SparseNet $[\oplus]$ always outperforms DenseNet with similar number of parameters. For example, DenseNet $N = 100, k = 12$ and SparseNet $[\oplus]$ $N = 100, k = 16, 32, 64$ both have around 7.2 million parameters but the latter shows better performance. DenseNet $N = 40, k = 12$ consumes around 1.1 million parameters but still has slightly worse Performance than SparseNet $[\oplus]$ with $N = 40, k = 12$.

Counterexamples do exist, such as the comparison between SparseNet $[\oplus]$ -BC-100- $\{32, 64, 128\}$ and DenseNet-BC-250-24. The latter model performs slightly better than the previous one with less parameters (17.71 vs 17.53). We argue this is an example of performance saturation considering DenseNet-BC-190-40 only has slightly higher accuracy than DenseNet-BC-250-24 with much more parameters (25.6 million vs 15.3 million), and it should result from the nature of the task of image classification on the CIFAR-100 dataset (17.53 vs 17.6).

Note that when we double the number of filters across different stage, the performance of SparseNets is greatly boosted and the better parameter of SparseNets $[\oplus]$ over DenseNet becomes more obvious. SparseNets $[\oplus]$ achieve similar or better performance than DenseNet while requiring at most half the number of parameters uniformly across all settings. These two general trends are summarized in the parameter-performance plot in Figure 2.

4.5 Results on ImageNet

Model	Error	Params	FLOPs	Time
DenseNet-121-32 [7]	25.0*	7.98M	5.7G	19.5ms
DenseNet-169-32 [7]	23.6*	14.15M	6.76G	32.0ms
DenseNet-201-32 [7]	22.5*	20.01M	8.63G	42.6ms
SparseNet $[\oplus]$ -121-32	25.6	4.51M	3.46G	13.5ms
SparseNet $[\oplus]$ -169-32	24.2	6.23M	3.74G	18.8ms
SparseNet $[\oplus]$ -201-32	23.1	7.22M	4.13G	22.0ms
SparseNet $[\oplus]$ -201-48	22.1	14.91M	9.19G	43.1ms
ResNet-50	23.9	25.5M	8.20G	42.2ms
ResNet-50 Pruned [37]	23.7	7.47M	-	-

Table 4. ImageNet results. The top-1 single-crop validation error, parameters, FLOPs, and time of each model on ImageNet.

We further test SparseNets $[\oplus]$ with different configurations and compare them with state-of-the-art networks on ImageNet to demonstrate its efficiency on a larger-scale dataset. All models are trained with same preprocessing methods and hyperparameters. Table 4 reports ImageNet validation error.

These results reveal the better parameter-performance efficiency of SparseNet $[\oplus]$ over DenseNet extends to ImageNet [31]: SparseNet $[\oplus]$ performs similarly to state-of-the-art DenseNets while requiring significantly fewer parameters. For example, SparseNet-201-48 (14.91M) yields better validation error than DenseNet-201-32 (20.01M). SparseNet-201-32 (7.22M) outperformed DenseNet-169-32 with only half of the parameters.

Even compared to pruned networks, SparseNets shows competitive parameter efficiency. In the last row of the Table 4, we show the result of pruned ResNet using Deep Compression [37], whose parameter-performance efficiency significantly outperforms the unpruned ResNet-50. However, our SparseNet $[\oplus]$ -201-32 trained-from-scratch even has better error rate than pruned ResNet-50 with fewer parameters. See Figure 2 (left) for a complete efficiency plot.

4.6 Feature Reuse and Parameter Redundancy

The original DenseNets work [7] conducts a simple experiment to investigate how well a trained network reuses features across layers. In short, for layer ℓ in each densely connected block, they compute the average absolute weights of the part of the filters that convolves with each previous layer’s feature. The averaged absolute weights are rescaled between 0 and 1 for each layer ℓ . The k^{th} normalized value implies the relative dependency of the feature of layer ℓ on the feature of layer k , compared to other layers. The experiments are performed on a DenseNet consisting of 3 blocks with $l = 40$ and $k = 12$. We perform a similar experiment on a SparseNet model with the same configuration. We plot results as heat maps in Fig. 3. We also include the heat maps of the experiment on DenseNets [7] for comparison.

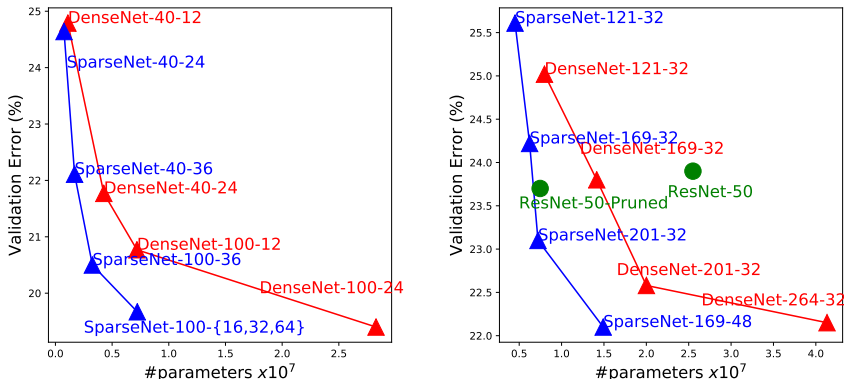


Fig. 2. Parameter efficiency. Comparison between DenseNets and SparseNets \oplus on top-1% error and number of parameters with different configurations. **Left:** CIFAR. **Right:** ImageNet. SparseNets achieve lower error with fewer parameters.

In this heap map, a red pixel at location (ℓ, k) indicates layer ℓ makes heavy use of the features of layer k and a blue pixel indicates relatively little usage. A white pixel indicates there is no direct connection between layer ℓ and layer k . We make the following observations from the heat maps:

- Most of the non-white pixels in the heat map of SparseNet are close to red, indicating that each layer takes full advantage of all the features it directly aggregates. It also indicates almost all the parameters are fully exploited, leaving little parameter redundancy. This result is not surprising considering the high parameter-performance efficiency of our model.
- In general, the pixel value at position (ℓ, k) in DenseNets decreases as the offset between ℓ and k gets larger. However, such a decaying trend does not appear in the heat map of SparseNets, implying that layers in SparseNets have better ability to extract useful features from long-distance connections to preceding layers.

5 Conclusion

We demonstrate that following a simple design rule, scaling aggregation link complexity in a logarithmic manner with network depth, yields a new state-of-the-art CNN architecture. Extensive experiments on CIFAR and ImageNet show our SparseNets offer significant efficiency improvements over the widely used ResNets and DenseNets. This increased efficiency allows SparseNets to scale robustly to great depth. While CNNs have recently moved from the 10-layer to 100-layer regime, perhaps new possibilities will emerge with straightforward and robust training of 1000-layer networks.

The performance of neural networks for visual recognition has grown with their depth as they evolved from AlexNet [1] to ResNet [5,6]. Extrapolating such

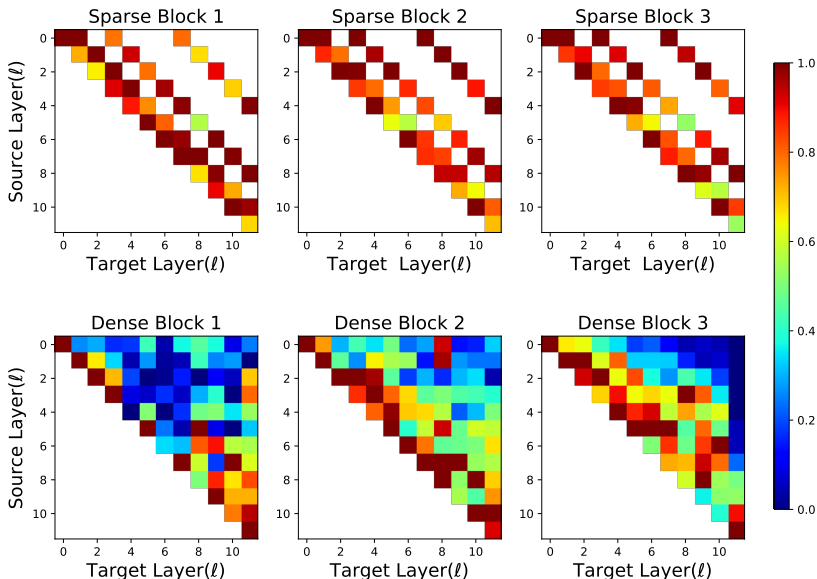


Fig. 3. The average absolute filter weights of convolutional layers in trained DenseNet and SparseNet. The color of pixel (s, ℓ) indicates the average weights of connection from layer s to ℓ within a block. The first row encodes the weights attached to the first input layer of a DenseNet/SparseNet Block.

trends could be cause to believe building deeper networks should further improve performance. Much effort has been devoted by researchers in computer vision and machine learning communities to train deep neural networks with more than 1000 layers, with such hope [6,38].

Though previous works and our experiments show we can train a very deep neural networks with stochastic gradient descent, their test performance still usually plateaus. Even so, very deep neural networks might be suitable for other interesting tasks. One possible direction could be solving sequential reasoning tasks relying on long-term dependencies. Skip connections would empower the network with the backtracking ability. Sparse feature aggregation could permit building extremely deep neural networks for such tasks.

References

1. Krizhevsky, A., Sutskever, I., Hinton, G.E.: Imagenet classification with deep convolutional neural networks. In: Advances in neural information processing systems. (2012) 1097–1105
2. Simonyan, K., Zisserman, A.: Very deep convolutional networks for large-scale image recognition. arXiv preprint arXiv:1409.1556 (2014)

3. Szegedy, C., Liu, W., Jia, Y., Sermanet, P., Reed, S., Anguelov, D., Erhan, D., Vanhoucke, V., Rabinovich, A.: Going deeper with convolutions. In: Proceedings of the IEEE conference on computer vision and pattern recognition. (2015) 1–9
4. Szegedy, C., Ioffe, S., Vanhoucke, V., Alemi, A.A.: Inception-v4, inception-resnet and the impact of residual connections on learning. In: AAAI. (2017) 4278–4284
5. He, K., Zhang, X., Ren, S., Sun, J.: Deep residual learning for image recognition. In: Proceedings of the IEEE conference on computer vision and pattern recognition. (2016) 770–778
6. He, K., Zhang, X., Ren, S., Sun, J.: Identity mappings in deep residual networks. ECCV (2016)
7. Huang, G., Liu, Z., Weinberger, K.Q., van der Maaten, L.: Densely connected convolutional networks. arXiv preprint arXiv:1608.06993 (2016)
8. Girshick, R., Donahue, J., Darrell, T., Malik, J.: Rich feature hierarchies for accurate object detection and semantic segmentation. In: Computer Vision and Pattern Recognition. (2014)
9. He, K., Gkioxari, G., Dollar, P., Girshick, R.: Mask R-CNN. ICCV (2017)
10. Long, J., Shelhamer, E., Darrell, T.: Fully convolutional networks for semantic segmentation. CVPR (2015)
11. Chen, L.C., Papandreou, G., Kokkinos, I., Murphy, K., Yuille, A.L.: Deeplab: Semantic image segmentation with deep convolutional nets, atrous convolution, and fully connected CRFs. arXiv:1606.00915 (2016)
12. Zhao, H., Shi, J., Qi, X., Wang, X., Jia, J.: Pyramid scene parsing network. CVPR (2017)
13. Larsson, G., Maire, M., Shakhnarovich, G.: FractalNet: Ultra-deep neural networks without residuals. ICLR (2017)
14. Ioffe, S., Szegedy, C.: Batch normalization: Accelerating deep network training by reducing internal covariate shift. In: International Conference on Machine Learning. (2015) 448–456
15. Iandola, F.N., Moskewicz, M.W., Ashraf, K., Han, S., Dally, W.J., Keutzer, K.: SqueezeNet: AlexNet-level accuracy with 50x fewer parameters and <1MB model size. arXiv:1602.07360 (2016)
16. Xie, S., Girshick, R., Dollár, P., Tu, Z., He, K.: Aggregated residual transformations for deep neural networks. arXiv preprint arXiv:1611.05431 (2016)
17. Huang, G., Liu, S., van der Maaten, L., Weinberger, K.Q.: CondenseNet: An efficient densenet using learned group convolutions. CVPR (2018)
18. Chen, W., Wilson, J.T., Tyree, S., Weinberger, K.Q., Chen, Y.: Compressing neural networks with the hashing trick. CoRR **abs/1504.04788** (2015)
19. Long, J., Shelhamer, E., Darrell, T.: Fully convolutional networks for semantic segmentation. In: Proceedings of the IEEE Conference on Computer Vision and Pattern Recognition. (2015) 3431–3440
20. Hariharan, B., Arbelaez, P., Girshick, R., Malik, J.: Hypercolumns for object segmentation and fine-grained localization. CVPR (2015)
21. Badrinarayanan, V., Kendall, A., Cipolla, R.: SegNet: A deep convolutional encoder-decoder architecture for image segmentation. arXiv:1511.00561 (2015)
22. Ronneberger, O., Fischer, P., Brox, T.: U-Net: Convolutional networks for biomedical image segmentation. arXiv:1505.04597 (2015)
23. Lee, C.Y., Xie, S., Gallagher, P., Zhang, Z., Tu, Z.: Deeply-supervised nets. AIS-TATS (2015)
24. Srivastava, R.K., Greff, K., Schmidhuber, J.: Highway networks. arXiv preprint arXiv:1505.00387 (2015)

25. tZoph, B., Le, Q.V.: Neural architecture search with reinforcement learning. arXiv preprint arXiv:1611.01578 (2016)
26. Hu, H., Dey, D., Giorno, A.D., Hebert, M., Bagnell, J.A.: Log-densenet: How to sparsify a densenet. CoRR **abs/1711.00002** (2017)
27. Greff, K., Srivastava, R.K., Schmidhuber, J.: Highway and residual networks learn unrolled iterative estimation. ICLR (2017)
28. Wang, W., Li, X., Yang, J., Lu, T.: Mixed link networks. CoRR **abs/1802.01808** (2018)
29. Chen, Y., Li, J., Xiao, H., Jin, X., Yan, S., Feng, J.: Dual path networks. CoRR **abs/1707.01629** (2017)
30. Krizhevsky, A., Hinton, G.: Learning multiple layers of features from tiny images. (2009)
31. Deng, J., Dong, W., Socher, R., Li, L.J., Li, K., Fei-Fei, L.: Imagenet: A large-scale hierarchical image database. In: Computer Vision and Pattern Recognition, 2009. CVPR 2009. IEEE Conference on, IEEE (2009) 248–255
32. Paszke, A., Chintala, S., Collobert, R., Kavukcuoglu, K., Farabet, C., Bengio, S., Melvin, I., Weston, J., Mariethoz, J.: Pytorch: Tensors and dynamic neural networks in python with strong gpu acceleration, may 2017
33. He, K., Zhang, X., Ren, S., Sun, J.: Delving deep into rectifiers: Surpassing human-level performance on imagenet classification. In: Proceedings of the IEEE international conference on computer vision. (2015) 1026–1034
34. Gross, S., Wilber, M.: Training and investigating residual nets. (2016)
35. Zagoruyko, S., Komodakis, N.: Wide residual networks. CoRR **abs/1605.07146** (2016)
36. Larsson, G., Maire, M., Shakhnarovich, G.: Fractalnet: Ultra-deep neural networks without residuals. CoRR **abs/1605.07648** (2016)
37. Han, S., Mao, H., Dally, W.J.: Deep compression: Compressing deep neural networks with pruning, trained quantization and huffman coding. arXiv preprint arXiv:1510.00149 (2015)
38. Huang, G., Sun, Y., Liu, Z., Sedra, D., Weinberger, K.Q.: Deep networks with stochastic depth. In: European Conference on Computer Vision, Springer (2016) 646–661